

# Shifting hail hazard under global warming

Timothy H. Raupach<sup>1,2\*</sup>, Raphael Portmann<sup>3</sup>, Christian Siderius<sup>4</sup>,  
Steven C. Sherwood<sup>1,2</sup>

<sup>1</sup>Climate Change Research Centre, UNSW Sydney, Mathews Building  
Level 4, The University of New South Wales, Sydney, 2051, NSW,  
Australia.

<sup>2</sup>ARC Centre of Excellence for Climate Extremes, UNSW Sydney,  
Australia.

<sup>3</sup>Agroscope, Swiss Federal Office for Agriculture, Zurich, Switzerland.

<sup>4</sup>Uncharted Waters Research, Sydney, Australia.

\*Corresponding author(s). E-mail(s): [timothy.h.raupach@gmail.com](mailto:timothy.h.raupach@gmail.com);

## Abstract

**Keywords:** hail, severe weather, convection, trends, projections

Hailstorms are extreme weather that cause significant damage to assets and crop losses worldwide. Hail and the storms that produce it are expected to be affected by anthropogenic global warming, yet regional studies using observations or projections show geographical inhomogeneities and there remains high uncertainty on the details of any changes [1]. Globally, hail observations are scarce[1], meaning global climatologies generally rely on satellite data [2, 3] or examination of environmental conditions in reanalyses using hail proxies [4]. Here, we provide the first global projections of future hail hazard, using a hail proxy applied to model output from the Coupled Model Intercomparison Project (CMIP6) [5] in a per-degree framework.

## Results

### Comparison to ERA5 for historical period

Figure 1 shows a comparison between the multi-model, multi-proxy mean of annual hail-prone days for the CMIP6 models, and the multi-proxy mean of annual hail-prone

days for the ERA5 reanalyses. Supplementary Figure 1 shows mean annual hail-prone days for the individual models and ERA5 for each proxy. While the CMIP6 models show a wide spread of absolute values, the locations of hail hotspots match well between reanalysis and models. The models MPI-ESM1-2-HR and EC-Earth show similar numbers of hail-prone days to ERA5, while MIROC6, CMCC-CM2-SR5, and CMCC-ESM2 show moderately more and CNRM-CM6-1 and GISS-E2-1-G show significantly more hail activity than ERA5. There are also differences across the selected hail proxies, with the Significant Hail Parameter (SHIP) [6] producing the least hail-prone days and the proxy of Raupach et al. 2023 without extra conditions [7] producing the greatest number of hail-prone days. Given the geographical agreement but differences in absolute numbers of hail-prone days, we consider relative changes per model in the rest of our analyses.

## Case study hail-prone day anomalies

Figure 2 shows multi-proxy mean monthly anomalies in proxy-derived hail-prone days for months with known high occurrences of damaging hailstorms. The proxy produced higher than average numbers of hail-prone days for February 2015 in northern and central India, regions that were affected by hailstorms that caused major losses to wheat crops at this time [8]. Similarly the proxy highlights areas of central and southern Europe as particularly hail-prone in June 2022, when the passage of two low-pressure systems caused hailstorm outbreaks across these regions [9] that broke records for insured losses in France [10]. The proxy also identified April 2015 and October 2022 as unusually hail-prone months in northeast India and western France, respectively (Supplementary Figures 2 and 3); there were reported hailstorms in both regions during the respective months [9, 11]. These case-study results increase our confidence in the ability of the proxy, which was trained using data from Australia [7], to identify hail-prone conditions worldwide.

## Changes in hail-prone days with warming

Figure 3 and Figure 4 show multi-model mean relative changes for the northern winter months and northern summer months, respectively. Relative differences for each model individually are shown in Supplementary Material Figures 6 and 7. Multi-model mean differences for all seasons are shown in Supplementary Material Figures 8 and 9.

There is a general decrease of hail-prone days in warmer regions and in summer, and an increase in cooler regions and in winter. The changes are stronger with greater warming. In the northern winter months there are increases projected for North America, southeastern Europe, Japan, and Tasmania, with decreases across southern Mexico, Central America, the Caribbean, regions in South America including Argentina, tropical western Africa, eastern South Africa, eastern India, and northern Australia. In the northern summer, there are decreases in hail-prone days projected for southeastern North America, Europe and northern Africa, the Sahara, northeastern China, while increases are projected in northeastern Canada, Tasmania, and the arctic north.

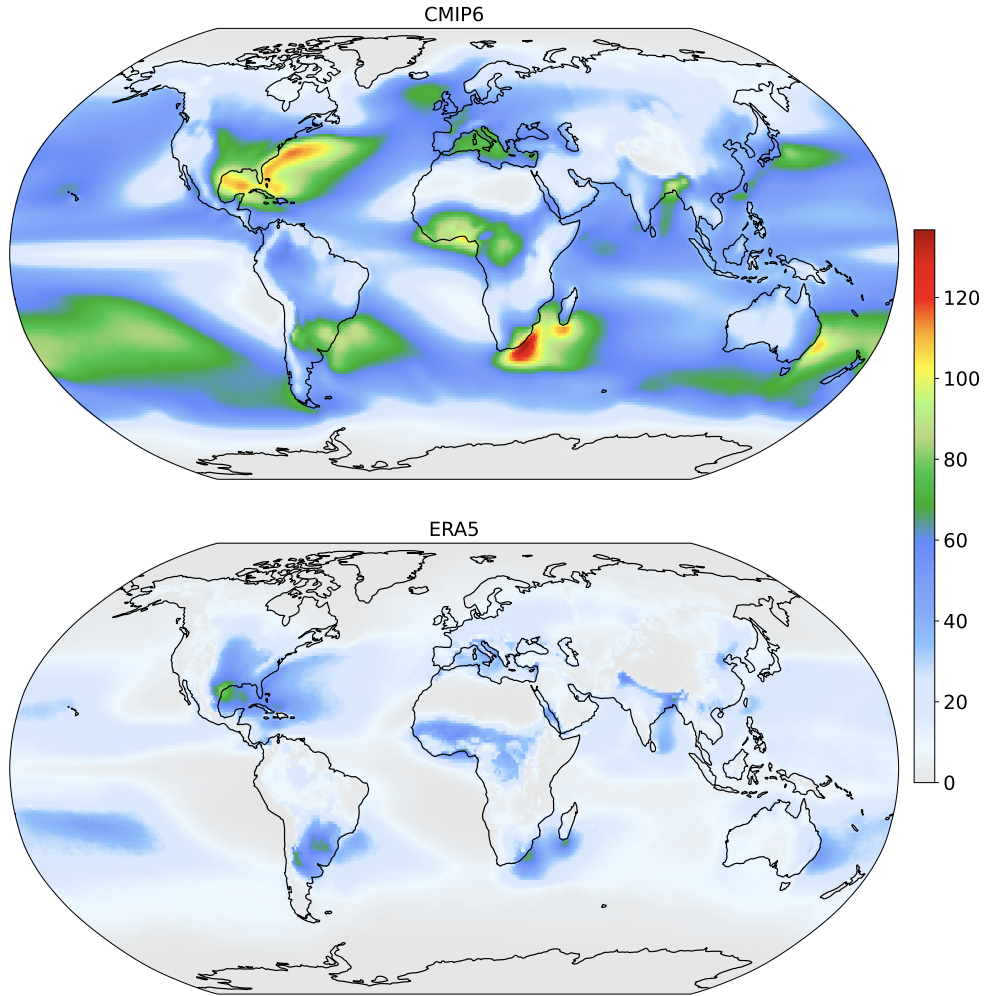
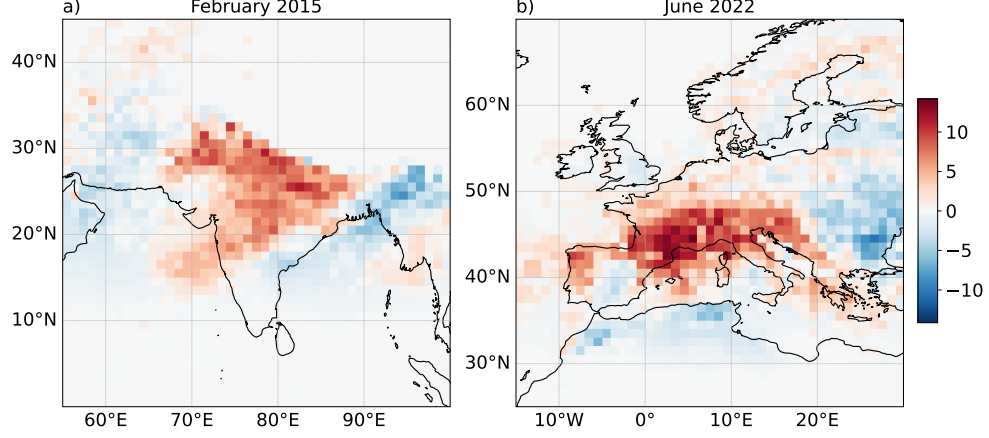


Fig. 1 Multi-model, multi-proxy mean annual hail-prone days for CMIP6 models, and multi-proxy mean annual hail-prone days for ERA5 reanalysis, for four selected proxies over the historical period (1980-1999) at  $1 \times 1^\circ$  resolution.

### Changes in atmospheric ingredients for hail

Figure 5 shows relative changes in atmospheric ingredients for hail for the  $3^\circ$  warming scenario. Supplementary Material Figure 10 shows the relative changes for ingredients in the  $2^\circ$  scenario.



**Fig. 2 Hail-proxy monthly anomalies highlight known hail-prone periods.** Colours show the monthly anomaly in proxy-derived hail-prone days in ERA5 data with respect to the monthly historical climatology (1980-1999), for a) the Indian subcontinent in February 2015 and b) Europe in June 2022. Anomalies for all months in these selected years are shown for the Indian subcontinent and Europe in Supplementary Figures 2 and 3, respectively.

## Changes in hail-prone days in cropping periods

### Methods

#### Data

We used a filtering approach to select models from the Coupled Model Intercomparison Project Phase 6 (CMIP6) [5]. We selected models that contained variables required to calculate convective indices: air temperature at the surface (**tas**) and by model level (**ta**), wind vectors at the surface (**uas** and **vas**) and by level (**ua** and **va**), specific humidity at the surface (**huss**) and by level (**hus**), and surface pressure (**ps**). We filtered for models with a temporal resolution higher than six-hourly (those with “table IDs” of **3hr** or **6hrLev**), and models that were available for both historical and SSP5-8.5 experiments (“experiment IDs” of **historical** or **ssp585**). Further, the models had to be available in the National Computational Infrastructure (NCI) node of the Earth System Grid Federation (ESGF), and had to cover the required epochs. The resulting CMIP6 models, that we used here, are detailed in Supplementary Material Table 1. If model orography was available in the **orog** variable, it was used; if not, the orography of the historical runs of CNRM-CM6-1 (ensemble **r1i1p1f2**) was interpolated onto the model grid and used instead [12]. Reanalyses were European Centre for Medium-range Weather Forecasts (ECMWF) reanalysis 5 (ERA5) data [13] on pressure levels [14]. To match the CMIP6 model characteristics, we used global ERA5 data at 00, 06, 12, and 18 UTC for each day from 1980–1999, interpolated to  $1 \times 1^\circ$  resolution.

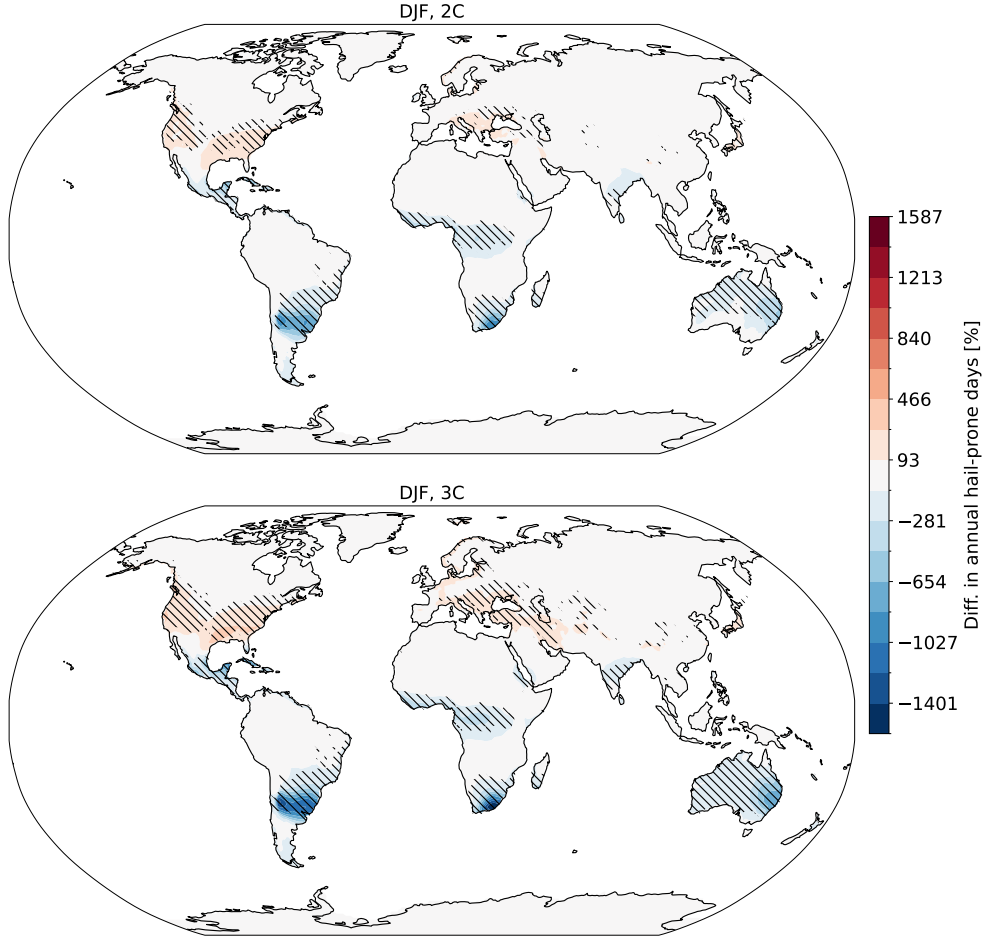


**Fig. 3 Changes in hail days for northern winter (December, January, and February).** Stippling shows regions in which at least 50% of the models agreed with the sign of the mean difference and also showed significant differences in the mean ( $p < 0.05$  on a t-test on two related samples).

## Application of hail proxies

We applied four hail-specific instability-shear proxies to CMIP6 and ERA5 data. The proxies were those of Raupach et al., 2023 (with and without “extra conditions” to remove false positives) [7], Eccel et al., 2012 [15], and a thresholds of 0.1 on the Significant Hail Parameter (SHIP) [6]. The proxies of Kunz 2007 [16] and Mohr and Kunz, 2013 [17] were tested but were found to produce unrealistically many hail-prone days in tropical regions for which they were not trained [7] (Supplementary Figure 5). Similarly, the threshold of 0.5 on SHIP, as has been used in other studies [4], was found to produce too few hail-prone days in comparison with the other proxy results (Supplementary Figure 5). Convective parameters were calculated as described for proxy of Raupach et al., 2023 [7], for each CMIP6 dataset at its native resolution and

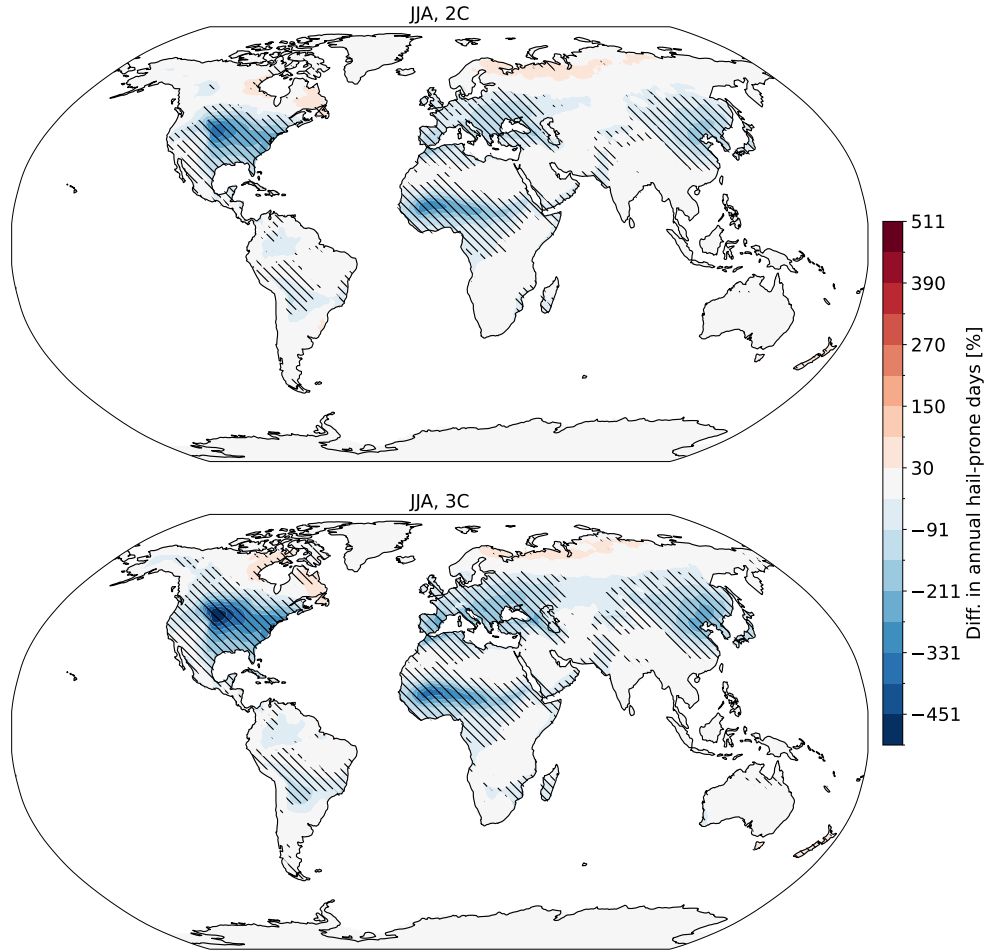


**Fig. 4** Changes in hail days for northern summer (June, July and August). As for Figure 3 but for the northern summer.

to ERA5 at the downscaled resolution. For each CMIP6 model, annual and seasonal statistics were calculated, then all statistics were interpolated onto a  $1 \times 1^\circ$  spatial grid for comparison.

### Per-degree framework

The historical period used for each model was 1980–1999. The epochs that represented  $2^\circ\text{C}$  and  $3^\circ\text{C}$  warming compared to the historical period were determined per model using 20-year running means of monthly global average temperature anomalies. The date ranges for each epoch are plotted in Supplementary Material Figure 4.

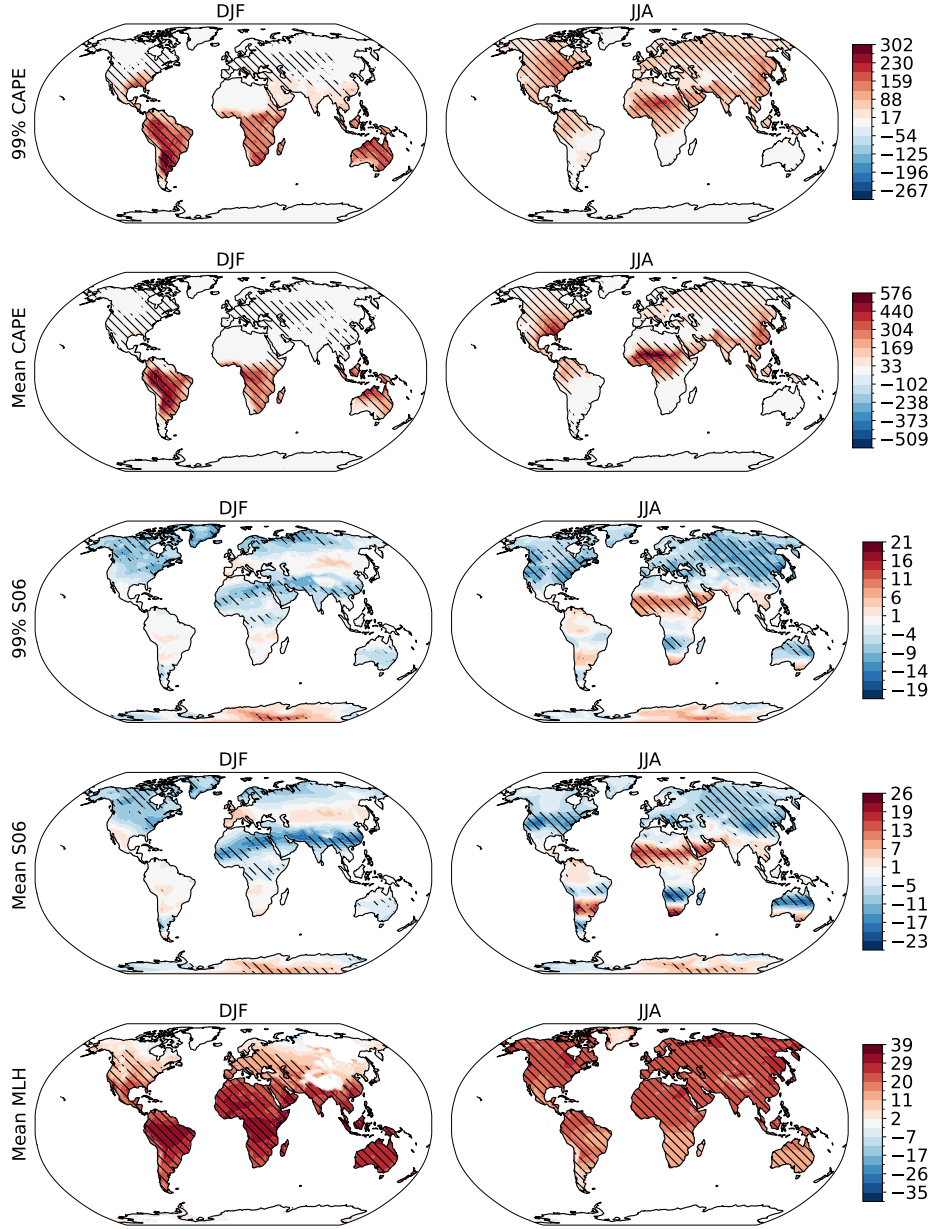


Fig. 5 Multi-model mean relative differences in hail ingredients for 2 C warming.

## Discussion

Although we show proxy results globally, the proxy of Raupach et al., 2023 was trained using land-based reports [7] and there is uncertainty in the occurrence of hail in maritime storms [18].

Leung et al., 2023 also observed a northward shift in hailstorms in the US from 2000 (preprint at [https://assets.researchsquare.com/files/rs-3217821/v1\\_covered\\_a256d1b8-b2e0-41b6-ab9c-e2628059bc91.pdf?c=1699615569](https://assets.researchsquare.com/files/rs-3217821/v1_covered_a256d1b8-b2e0-41b6-ab9c-e2628059bc91.pdf?c=1699615569).)

**Data availability.** MIRCA2000 data are available with identifier <https://doi.org/10.5281/zenodo.7422506>.

**Code availability.** Convective indices were calculated using `xarray_parcel` by T. H. Raupach (<https://doi.org/10.5281/zenodo.8088497>) (**Update version with new xarray release**). Warming levels were calculated using code by T. H. Raupach (**ref**).

**Acknowledgments.** This research was undertaken with the assistance of resources and services from the NCI, which is supported by the Australian Government.

**Competing interests.** The authors declare no competing financial or non-financial interests.

**Author contributions.**

## References

- [1] Raupach, T. H. *et al.* The effects of climate change on hailstorms. *Nat. Rev. Earth Environ.* **2**, 213–226 (2021).
- [2] Cecil, D. J. & Blankenship, C. B. Toward a global climatology of severe hailstorms as estimated by satellite passive microwave imagers. *J. Climate* **25**, 687–703 (2012).
- [3] Bang, S. D. & Cecil, D. J. Constructing a multifrequency passive microwave hail retrieval and climatology in the GPM domain. *J. Appl. Meteorol.* **58**, 1889–1904 (2019).
- [4] Prein, A. F. & Holland, G. J. Global estimates of damaging hail hazard. *Weather Clim. Extremes* **22**, 10–23 (2018).
- [5] Eyring, V. *et al.* Overview of the Coupled Model Intercomparison Project Phase 6 (CMIP6) experimental design and organization. *Geosci. Model Dev.* **9**, 1937–1958 (2016).
- [6] NOAA SPC. Significant hail parameter. [https://www.spc.noaa.gov/exper/mesoanalysis/help/help\\_sigh.html](https://www.spc.noaa.gov/exper/mesoanalysis/help/help_sigh.html) (2022). National Oceanographic and Atmospheric Administration National Weather Service Storm Prediction Center, accessed 21 June 2022.
- [7] Raupach, T. H., Soderholm, J., Protat, A. & Sherwood, S. C. An improved instability–shear hail proxy for australia. *Mon. Weather Rev.* **151**, 545–567 (2023).



- [8] Singh, S. K., Saxena, R., Porwal, A., Ray, N. & Ray, S. S. Assessment of hailstorm damage in wheat crop using remote sensing. *Curr Sci India* **112**, 2095–2100 (2017).
- [9] Pucik, T. Major hailstorms of 2022 (2023). URL <https://www.essl.org/cms/major-hailstorms-of-2022/>. Accessed 2024-01-10.
- [10] Soyka, T. Severe 2022 hail damage in france sets new benchmarks, underscores shift of risk and calls for pricing adjustments (2023). URL <https://www.swissre.com/risk-knowledge/mitigating-climate-risk/hail-damage-risk-france-2022.html>. Accessed 2024-01-10.
- [11] Chattopadhyay, N., Devi, S. S., John, G. & Choudhari, V. Occurrence of hail storms and strategies to minimize its effect on crops. *Mausam* **68**, 75–92 (2017).
- [12] Bracegirdle, T. J. *et al.* Twenty first century changes in Antarctic and Southern Ocean surface climate in CMIP6. *Atmos. Sci. Lett.* **21**, e984 (2020).
- [13] Hersbach, H. *et al.* The ERA5 global reanalysis. *Q. J. Roy. Meteor. Soc.* **146**, 1999–2049 (2020).
- [14] Hersbach, H. *et al.* ERA5 hourly data on pressure levels from 1979 to present (2018). Copernicus Climate Change Service (C3S) Climate Data Store (CDS).
- [15] Eccel, E., Cau, P., Riemann-Campe, K. & Biasioli, F. Quantitative hail monitoring in an alpine area: 35-year climatology and links with atmospheric variables. *Int. J. Climatol.* **3**, 503–517 (2012).
- [16] Kunz, M. The skill of convective parameters and indices to predict isolated and severe thunderstorms. *Nat. Hazards Earth Sys.* **7**, 327–342 (2007).
- [17] Mohr, S. & Kunz, M. Recent trends and variabilities of convective parameters relevant for hail events in Germany and Europe. *Atmos. Res.* **123**, 211–228 (2013).
- [18] Knight, C. A. & Knight, N. C. in *Hailstorms* (ed. Doswell, C. A.) *Severe Convective Storms* 223–254 (American Meteorological Society, Boston, MA, 2001).